GeoConvention
Calgary • Canada • March 7-11 2016
OPTIMIZING RESOURCES

PS and SP converted wave reflection coefficients and their application to time-lapse difference AVO

Shahin Jabbari: Ph.D. student at the University of Calgary, CREWES Project
Kristopher A. Innanen: Associate Professor at the University of Calgary, CREWES Project

Summary

Multicomponent time-lapse amplitude variation with offset (AVO) may improve approximating time-lapse seismic difference data. The difference data during the change in a reservoir from the baseline survey relative to the monitor survey are described for converted waves. A framework for linear and nonlinear time-lapse AVO difference data is formulated in order of the baseline interface contrast and time-lapse changes. The nonlinear higher order terms represent corrections appropriate for time-lapse problems especially for large contrasts cases. We conclude that in many plausible time-lapse scenarios the increase in accuracy associated with higher order corrections is non-negligible for converted wave. Furthermore the third order approximation terms in difference AVO emphasizes on the difference for exact reflection coefficient between SP and PS waves.

Introduction

The employment of enhanced oil recovery (EOR) techniques affects reservoir properties such as fluid flow and pressure. A time-lapse seismic survey allows us to monitor the production of hydrocarbons by measuring the changes in the behavior of a reservoir over time. Comparison of repeated seismic surveys over months, years, or decades adds a fourth dimension, calendar time, to the seismic data. In a time-lapse seismic survey the Baseline survey, which is acquired prior to production of a reservoir, is compared to the Monitor survey, acquired after a particular interval of time following several geological-geophysical reservoir changes. The difference between the Baseline survey and subsequent Monitor surveys can be analyzed to interpret changes in the reservoir (Greaves and Fulp 1987, Lumley 2001, Landrø 2001). Perturbation (scattering) theory and amplitude variation with offset (AVO) methods can be used to model and invert the difference data in a time-lapse survey. The Baseline survey describes the background medium against which we measure the perturbation detected in the Monitor survey. The perturbation quantifies the changes in P-wave and S-wave velocities and density between the times of the Baseline and Monitor surveys (Stolt 2012, Innanen 2014).

Although P-wave seismic is the primary survey method in seismology, using multicomponent recording can improve and support P-wave seismic data, especially for rocks with similar P-wave properties which may show a greater variation in S-wave properties. Multicomponent surveying has been developed rapidly in both land and marine acquisition and processing techniques, with many applications in structural imaging, lithologic estimation, anisotropy analysis, and reservoir monitoring. The elastic properties of a rock, as well as acoustic properties, change when the pressure and fluid flow is altered in a reservoir due to production. This raise the necessity of multicomponent 4D time-lapse analysis in a reservoir (Stewart et al. 2002 and 2003).

Time-lapse amplitude variation with offset (time-lapse AVO) connotes the analysis of changes to the offset or angle dependence of reflection coefficients from the baseline to the monitor survey. A framework has been formulated to model linear and nonlinear elastic time-lapse AVO difference for P-P sections (Jabbari et al. 2015). The study described here focuses on applying linear and nonlinear time-lapse amplitude variation with offset methods to model the difference data for converted wave and more specifically to investigate the deference between SP and PS wave in nonlinearity.

Theory

Our time-lapse survey consists of two seismic experiments; a Baseline survey followed by a Monitor survey. We consider an incident P or S wave striking the boundary between two elastic media which are incidence medium and reservoir with rock properties V_{P0}, V_{S0}, ρ_0 (above) and V_{PBL}, V_{SBL}, ρ_{BL} (below). The reservoir properties change to V_{PM}, V_{SM}, ρ_M in the Monitor survey. Amplitudes of reflected and transmitted P and S waves are calculated through setting the boundary conditions in the Zoeppritz equations which can be rearranged in matrix form e.g. (Keys 1989):

$$P_{BL}\begin{bmatrix} R_{PP} \\ R_{PS} \\ T_{PP} \\ T_{PS} \end{bmatrix} = b_{BL} \quad R_{PS}^{BL}(\theta) = \frac{\det(P_P)}{\det(P)} \qquad P_{M}\begin{bmatrix} R_{PP} \\ R_{PS} \\ T_{PP} \\ T_{PS} \end{bmatrix} = b_{M} \quad R_{PS}^{M}(\theta) = \frac{\det(P_P)}{\det(P)}$$

$$S_{BL}\begin{bmatrix} R_{SS} \\ R_{SP} \\ T_{SS} \\ T_{SP} \end{bmatrix} = c_{BL} \quad R_{SP}^{BL}(\varphi) = \frac{\det(S_S)}{\det(S)} \qquad S_{M}\begin{bmatrix} R_{SS} \\ R_{SP} \\ T_{SS} \\ T_{SP} \end{bmatrix} = c_{M} \quad R_{SP}^{M}(\varphi) = \frac{\det(S_S)}{\det(S)}$$

Where P_{BL} P_M, S_{BL}, and S_M are Zoeppritz metrics for the Baseline and Monitor survey for incident P and incident S wave. P_P, S_S are the P and S metrics with the second column replaced by the vector b_{BL}, c_{BL}, b_M, and c_M respectively. R's and T's are reflection and transmission coefficients for PS and SP waves.

In our time-lapse study we have considered two groups of perturbation parameters; perturbations "b" representing the change from the incidence medium to the target medium in the baseline survey, and perturbations "a" representing target medium changes from the baseline to monitor survey:

$$b_{VP} = 1 - \frac{V_{P0}^2}{V_{PBL}^2}, \quad b_{VS} = 1 - \frac{V_{S0}^2}{V_{SBL}^2}, \quad b_{\rho} = 1 - \frac{\rho_0}{\rho_{BL}}, \qquad a_{VP} = 1 - \frac{V_{PBL}^2}{V_{PM}^2}, \quad a_{VS} = 1 - \frac{V_{SBL}^2}{V_{SM}^2}, \quad a_{\rho} = 1 - \frac{\rho_{BL}}{\rho_M},$$

Substituting these perturbations into the two requisite instances of the Zoeppritz equations (modeling the Baseline and the Monitor reflection amplitudes), we derive a series expansion for the difference data reflection as follows.

$$\Delta R_{PS}(\theta) = R_{PS}^{(M)}(\theta) - R_{PS}^{(BL)}(\theta) \qquad \Delta R_{SP}(\varphi) = R_{SP}^{(M)}(\varphi) - R_{SP}^{(BL)}(\varphi)$$

$$\Delta R_{PS}(\theta) = \Delta R_{PS}^{(1)}(\theta) + \Delta R_{PS}^{(2)}(\theta) + \Delta R_{PS}^{(3)}(\theta) + \ldots \qquad \Delta R_{SP}(\varphi) = \Delta R_{SP}^{(1)}(\varphi) + \Delta R_{SP}^{(2)}(\varphi) + \Delta R_{SP}^{(3)}(\varphi) + \ldots$$

where θ and φ are P and S waves incident angles on the interface between the cap rock and reservoir.

Results

Linear and higher order terms for PS and SP are presented in the next page. Investigating third order equations shows that the third order terms are different for PS and SP converted waves. This difference emphasizes that, the difference between PS and SP reelection coefficient can be verified by higher order approximations as the linear and second order terms are identical.

Numerical examples

In this section, we examine the derived linear and nonlinear difference time-lapse AVO terms for PS converted wave and SP converted wave qualitatively with numerical examples. In the first example, the data used by Landrø (2001) are applied. Typical values for P-wave and S-wave velocities and density for

$$\Delta R_{PS}^{(1)}(\theta) = \left[-\frac{V_{S_0}}{V_{P_0}}\sin\theta\right] a_{VS} + \left[-\frac{1}{2}\left(2\frac{V_{S_0}}{V_{P_0}}+1\right)\sin\theta\right] a_\rho$$

$$\begin{aligned}\Delta R_{PS}^{(2)}(\theta) = &\left[-\frac{3}{4}\frac{V_{S_0}}{V_{P_0}}\sin\theta\right] a_{VS}^2 + \left[-\frac{1}{2}\sin\theta\right] a_\rho^2 + \left[\frac{1}{2}\left(2\frac{V_{S_0}}{V_{P_0}}-1\right)\sin\theta\right] b_\rho a_\rho \\ &+ \left[-\frac{1}{2}\frac{V_{S_0}}{V_{P_0}}\sin\theta\right] b_{VS} a_{VS} + \left[\frac{1}{4}\frac{V_{S_0}}{V_{P_0}}\sin\theta\right] (a_{Vp} a_{VS} + a_{Vp} b_{VS} + b_{Vp} a_{VS}) \\ &+ \left[\frac{1}{8}\left(2\frac{V_{S_0}}{V_{P_0}}-1\right)\sin\theta\right] (a_{Vp} a_\rho + b_\rho a_{Vp} + a_\rho b_{Vp} + a_\rho a_{VS} + a_\rho b_{VS} + b_\rho a_{VS})\end{aligned}$$

$$\begin{aligned}\Delta R_{PS}^{(3)}(\theta) = &\left[-\frac{5}{8}\frac{V_{S_0}}{V_{P_0}}\sin\theta\right] a_{VS}^3 + \left[\frac{1}{8}\left(2\frac{V_{S_0}}{V_{P_0}}-3\right)\sin\theta\right] a_\rho^3 + \left[-\frac{3}{8}\frac{V_{S_0}}{V_{P_0}}\sin\theta\right] \\ &(b_{VS} a_{VS}^2 + b_{VS}^2 a_{VS}) + \left[\frac{1}{16}\left(6\frac{V_{S_0}}{V_{P_0}}-1\right)\sin\theta\right] (a_\rho^2 a_{VS} + b_\rho^2 a_{VS} + a_\rho^2 b_{VS}) + \\ &\left[\frac{1}{16}\left(4\frac{V_{S_0}}{V_{P_0}}-1\right)\sin\theta\right] (a_\rho b_{VS}^2 + a_\rho a_{VS}^2 + b_\rho a_{VS}^2) + \left[\frac{1}{16}\left(2\frac{V_{S_0}}{V_{P_0}}-1\right)\right. \\ &\left.\sin\theta\right] (b_\rho a_{VP}^2 + b_\rho^2 a_{VP} + a_\rho b_{VP}^2 + a_\rho^2 b_{VP} + a_\rho^2 a_{VP} + a_\rho a_{VP}^2) + \\ &\left[\frac{1}{8}\frac{V_{S_0}}{V_{P_0}}\sin\theta\right] (b_{VP}^2 a_{VS} + a_{VP}^2 b_{VS} + a_{VP}^2 a_{VS} + b_{VP} b_{VS} a_{VS} + a_{VP} b_{VS} a_{VS}) \\ &+ \left[\frac{1}{8}\left(6\frac{V_{S_0}}{V_{P_0}}-1\right)\sin\theta\right] (b_\rho^2 a_\rho + b_\rho a_\rho^2) + \left[\frac{1}{32}\left(2\frac{V_{S_0}}{V_{P_0}}-1\right)\sin\theta\right] (a_\rho b_{VP} a_{VS} \\ &+ a_\rho b_{VP} b_{VS} + b_\rho a_{VP} a_{VS} + b_\rho a_{VP} b_{VS} + a_\rho a_{VP} a_{VS} + a_\rho a_{VP} b_{VS} + b_\rho b_{VP} a_{VS}) \\ &\left[\frac{1}{4}\frac{V_{S_0}}{V_{P_0}}\sin\theta\right] (b_\rho b_{VS} a_{VS} + a_\rho b_{VS} a_{VS}) + \left[\frac{1}{2}\frac{V_{S_0}}{V_{P_0}}\sin\theta\right] (b_\rho a_\rho a_{VS} + b_\rho a_\rho b_{VS}) \\ &+ \left[\frac{3}{16}\frac{V_{S_0}}{V_{P_0}}\sin\theta\right] (a_{VP} b_{VS}^2 + a_{VP} a_{VS}^2 + b_{VP} a_{VS}^2)\end{aligned}$$

$$\Delta R_{SP}^{(1)}(\phi) = \left[-\frac{V_{S_0}}{V_{P_0}}\sin\phi\right] a_{VS} + \left[-\frac{1}{2}\left(2\frac{V_{S_0}}{V_{P_0}}+1\right)\sin\phi\right] a_\rho$$

$$\begin{aligned}\Delta R_{SP}^{(2)}(\phi) = &\left[-\left(\frac{3}{4}\right)\frac{V_{S_0}}{V_{P_0}}\sin\phi\right] a_{VS}^2 + \left[-\frac{1}{2}\sin\phi\right] a_\rho^2 + \left[\frac{1}{2}\left(2\frac{V_{S_0}}{V_{P_0}}-1\right)\sin\phi\right] b_\rho a_\rho \\ &+ \left[-\left(\frac{1}{2}\right)\frac{V_{S_0}}{V_{P_0}}\sin\phi\right] b_{VS} a_{VS} + \left[\left(\frac{1}{4}\right)\frac{V_{S_0}}{V_{P_0}}\sin\phi\right] (a_{VP} a_{VS} + a_{Vp} b_{VS} + b_{Vp} a_{VS}) \\ &+ \left[\frac{1}{8}\left(2\frac{V_{S_0}}{V_{P_0}}-1\right)\sin\phi\right] (a_{Vp} a_\rho + b_\rho a_{Vp} + a_\rho b_{Vp} + a_\rho a_{VS} + a_\rho b_{VS} + b_\rho a_{VS})\end{aligned}$$

$$\begin{aligned}\Delta R_{SP}^{(3)}(\phi) = &\left[\left(\frac{3}{8}\right)\frac{V_{S_0}}{V_{P_0}}\sin\phi\right] a_{VS}^3 + \left[\frac{1}{8}\left(10\frac{V_{S_0}}{V_{P_0}}+1\right)\sin\phi\right] (a_\rho^3 + b_{VS} b_\rho a_{VS} + b_{VS} a_\rho a_{VS} \\ &+ b_\rho a_{VS}^2 + a_\rho a_{VS}^2 + a_\rho b_{VS}^2) + \left[\frac{1}{32}\left(2\frac{V_{S_0}}{V_{P_0}}-1\right)\sin\phi\right] (b_{VP} b_\rho a_{VS} + \\ &b_{VP} a_\rho a_{VS} + b_{VS} b_\rho a_{VP} + b_{VS} a_\rho a_{VP} + b_{VP} a_\rho b_{VS} + a_{VP} b_\rho a_{VS} + a_{VP} a_\rho a_{VS}) \\ &+ \left[\frac{1}{4}\left(6\frac{V_{S_0}}{V_{P_0}}+1\right)\sin\phi\right] (a_\rho b_\rho a_{VS} + a_\rho b_\rho b_{VS}) + \left[\frac{1}{16}\left(22\frac{V_{S_0}}{V_{P_0}}+3\right)\sin\phi\right] \\ &(a_{VS} a_\rho^2 + b_{VS} a_\rho^2 + a_{VS} b_\rho^2) + \left[\frac{1}{8}\left(14\frac{V_{S_0}}{V_{P_0}}+3\right)\sin\phi\right] (b_\rho a_\rho^2 + a_\rho b_\rho^2) \left[\frac{1}{16} + \right. \\ &\left.\left(2\frac{V_{S_0}}{V_{P_0}}-1\right)\sin\phi\right] (b_{VP} a_\rho^2 + a_{VP} b_\rho^2 + a_{VP} a_\rho^2 + a_{VP}^2 b_\rho + a_{VP}^2 a_\rho + b_{VP}^2 a_\rho) \\ &+ \left[\left(\frac{5}{8}\right)\frac{V_{S_0}}{V_{P_0}}\sin\phi\right] (a_{VS} b_{VS}^2 + b_{VS} a_{VS}^2) + \left[\left(\frac{1}{8}\right)\frac{V_{S_0}}{V_{P_0}}\sin\phi\right] (a_{VS} b_{VP}^2 + b_{VS} a_{VP}^2 \\ &+ a_{VS} a_{VP}^2 + a_{VS} b_{VS} a_{VP} + a_{VS} b_{VS} b_{VP}) + \left[\left(\frac{3}{16}\right)\frac{V_{S_0}}{V_{P_0}}\sin\phi\right] \\ &(b_{VP} a_{VS}^2 + a_{VP} b_{VS}^2 + a_{VP} a_{VS}^2)\end{aligned}$$

the cap rock and reservoir (preproduction and post production), which are taken from Gullfaks 4D project, are used. In the Gullfaks field, there are +13 %, -2 %, and +4 % changes in the reservoir in P-wave and S-wave velocities and density respectively due to the production. For the second example, we used data by Veire (2006). Veire used two synthetic models for the reservoir: a baseline scenario with a water saturation of 10 % and an effective pressure of 2 MPa . In the monitor survey, the water saturation and effective pressure are 50 % and 8 MPa respectively. These changes altered the seismic parameters and caused 15 %, 11 %, and 1 % increase respectively in P-wave and S-wave velocities and density.

We examined our formulation and compared them with the exact difference data. The theoretical results for PS and SP converted wave are examined for the dataset used by Landrø (2001) and Veire (2006):

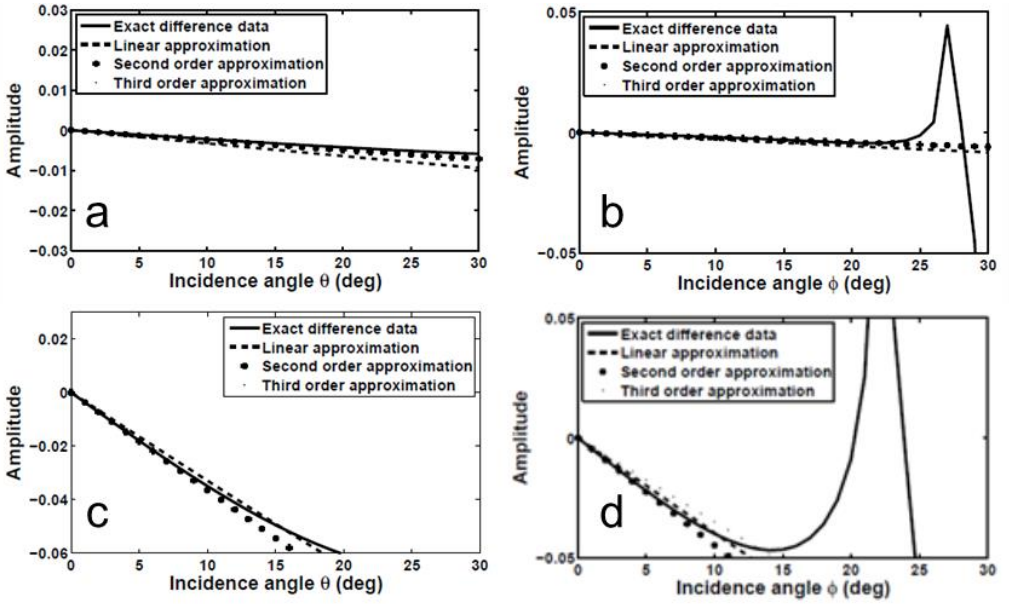

Figure 1: $\Delta R_{PS}(\theta)$ (a and c) and $\Delta R_{SP}(\varphi)$ (b and d) for the exact (Solid line), linear (- - -), second order (+++), and third order approximation (...). In (a) and (b) data set used by Landrø (2001) are applied. In (c) and (d) data used by Veire (2006) are applied.

Conclusions

A well-developed AVO regimes analysis converted wave and shear waves AVO as well the P-wave AVO. Jabbari et al. (2015) have already investigated P-wave time-lapse AVO and showen that adding the higher order terms in ΔR_{PP} to the linear approximation for difference time-lapse data increases the accuracy of the ΔR_{PP} and corrects the error due to linearization (Jabbari et al. 2015). This framework was extended by formulating a framework for the difference reflection data in ΔR_{PS}, ΔR_{SP}, and ΔR_{SS} (Jabbari and Innanen 2014 and 2015). In this study we focused on the difference between ΔR_{PS} and ΔR_{SP}. The results showed that, including higher order terms in ΔR for converted wave improves the accuracy of approximating time-lapse difference reflection data, particularly for large contrast cases. Comparing linear, second , and third order terms for ΔR_{PS} and ΔR_{SP} indicates their third roder terms are different. This confirms the difference between exact ΔR_{PS} and ΔR_{SP} which does not show up in the linear and second approximations.

Acknowledgements

We wish to thank sponsors, faculty, and staff of the Consortium for Research in Elastic Wave Exploration Seismology (CREWES) for their support of this work. We also gratefully acknowledge support from NSERC (Natural Science and Engineering Research Council of Canada) via two grants: CRDPJ 379744-08 and RGPIN 217032-2013.

References

Greaves, R. J., and Fulp, T. J., 1987, Three-dimensional seismic monitoring of an enhanced oil recovery process: Geophysics, 52, 1175–1187.

Keys, R. G., 1989, Polarity reversals in reflections from layered media: Geophysics, 54(7), 900–905.

Innanen, K. A., Naghizadeh, M., and Kaplan, S. T., 2014, Perturbation methods for two special cases of the time-lapse seismic inverse problem: Geophysical Prospecting, 62, 453–474.

Jabbari, S., Wong, J., and Innanen, K. A. (2015): A theoretical and physical modeling analysis of the coupling between baseline elastic properties and time-lapse changes in determining difference amplitude variation with offset: Geophysics, 80(6), N37-N48

Jabbari, S., and Innanen, K.A., 2013, A framework for approximation of elastic time-lapse difference AVO signatures and validation on physical modeling data: 75th EAGE Conference and Exhibition.

Jabbari, S., and Innanen, K.A., 2013, A framework for linear and nonlinear S-wave and C-wave time-lapse difference AVO: CREWES Annual Report.

Landrø, M., 2001, Discrimination between pressure and fluid saturation changes from time-lapse seismic data: Geophysics, 66(3), 836-844.

Lumley, D., 2001, Time-lapse seismic reservoir monitoring: Geophysics, 66(1), 50-53.

Stewart, R. R., Gaiser, J., Brown, R. J., and Lawton, D. C., 2003, Direct non-linear acoustic and elastic inversion: Tutorial: converted-wave seismic exploration: Application: Geophysics, 68(1), 40-57.

Stolt, R. H., and Weglein, A. B., 2012, Seismic Imaging and Inversion: Volume 1: Application of Linear Inverse Theory: Cambridge University Press. (use Arial 9pt normal)

Veire, H. H., Borgos H.G., and Landrø, M. 2006, Stochastic inversion of pressure and saturation changes from time-lapse AVO data: Geoscience, 71 (5), C81-C92.